Materials Advances

ROYAL SOCIETY OF CHEMISTRY

COMMUNICATION

View Article Online
View Journal | View Issue

Open Access Article. Published on 01 December 2022. Downloaded on 10/21/2025 6:40:41 AM.
This article is licensed under a Creative Commons Attribution 3.0 Unported Licence.

Check for updates

Cite this: *Mater. Adv.*, 2023, 4, 481

Received 7th October 2022,
Accepted 27th November 2022

DOI: 10.1039/d2ma00956k

rsc.li/materials-advances

Copper(I) iodide organic–inorganic hybrid luminescent inks for anti-counterfeiting application†

Hua Tong, Zhennan Zhou, Yi Lv, Haibo Li, Wei Liu * and Gangfeng Ouyang *

An efficient and universal method has been developed for the preparation of copper(I) iodide incorporated organic–inorganic hybrid coating materials. These materials exhibit potential as solvent-free anti-counterfeiting inks, with the advantages of facile prepration method, low-cost, uniform and bright light emissions, long service life, high stability, water resistance, and strong wearability.

Manufacturers today are increasingly seeking high-quality inks and coating materials to help produce products that are smaller, lighter, and more technologically advanced. Nowadays, anti-counterfeiting technology has strengthened information security protection by taking its unique advantages in photochemistry, electromagnetism, printing and spectral technology, *etc.* Modern anti-counterfeiting techniques include materials, digital information, printing technology, biological characteristics and other types of anti-counterfeiting methods.[1–3] Therefore, environmentally friendly luminescent inks with low toxicity, good optical performance, strong stability and mechanical performance are in great demand.

Organic–inorganic hybrid materials have rich structural types and can be used in a variety of areas, among which functional inks and coating materials are one of their important applications.[4–8] Organic–inorganic hybrid coatings are typically silicon oxide based resins, which are mainly prepared by sol–gel method.[9,10] In these hybrid materials, the inorganic component is silicon oxides, the organic components are polymers.[11] Such composite structures maintain the good hardness, scratch resistance, weather resistance properties from the inorganic species, and the flexibility, compactness and processability properties from the organic components.[9,12] Hybrid coating materials have many advantages, such as tunable structures and performance, facile synthesis and environmental friendliness, showing great potential for large-scale commercialization.[9,13]

With the improvement of living standards, coating materials are required to have more functions and specialties.[14–17] Luminescent coatings are one of the most important functional coatings since they can be used not only as decorative coatings, smart coatings, as well as anti-counterfeiting inks.[18–20] Silicon oxide based resins are generally non-luminescent, and lighting-emitting coating of this type are typically prepared by adding luminous substances such as phosphors and organic dye molecules into the resin materials.[20–23] Such mixing process is physical blending since there is no chemical bond between the added luminescent compounds and the coating materials, which may result in many problems, such as uneven luminescence distribution, and easy sedimentation of luminous particles, *etc.*[24,25]

Copper(I) iodide hybrid molecular clusters have excellent luminescence properties.[26–31] Generally, the reaction of copper(I) iodide with organic ligands leads to the formation of three types of structures, such as $Cu_2I_2(L)_x$ dimer based compounds, $Cu_4I_4(L)_x$ cubane based compounds, $CuI(L)_x$ staircase infinite chain based compounds.[32] Among them, $Cu_4I_4(L)_4$ cubane clusters are the most common in literature and demonstrate remarkable photoluminescence behavior.[33] Typically, 0D-$Cu_4I_4(L)_4$ molecular clusters emits strong yellow light under UV irradiation, with impressive internal quantum yields (IQYs) as high as 100%. Their emissions have been found to result from a cluster-centered (CC) mechanism, and is due to the strong Cu–Cu interaction within the Cu_4I_4 core.[34,35] A bottom-up precursor approach has been developed with the goal of keeping the inorganic core intact in the ligand-exchanged products.[36] Typically, a Cu_4I_4 based molecular cluster was selected as the precursor, and was well-dispersed in the solvent for ligand substitution. Through the: "bottom-up" method, small molecules with specific copper(I) iodide clusters can be used as precursors to controllably synthesize multi-dimensional hybrid structures with the identical inorganic cluster structure, and such multi-dimensional hybrid structures can typically

School of Chemical Engineering and Technology, Sun Yat-sen University, Zhuhai, 519082, Guangdong, P. R. China. E-mail: liuwei96@mail.sysu.edu.cn, cesoygf@mail.sysu.edu.cn

† Electronic supplementary information (ESI) available: Experimental details, structural plots of the coupling reagents, luminescent decay plot. See DOI: https://doi.org/10.1039/d2ma00956k

Open Access Article. Published on 01 December 2022. Downloaded on 10/21/2025 6:40:41 AM.
This article is licensed under a Creative Commons Attribution 3.0 Unported Licence.

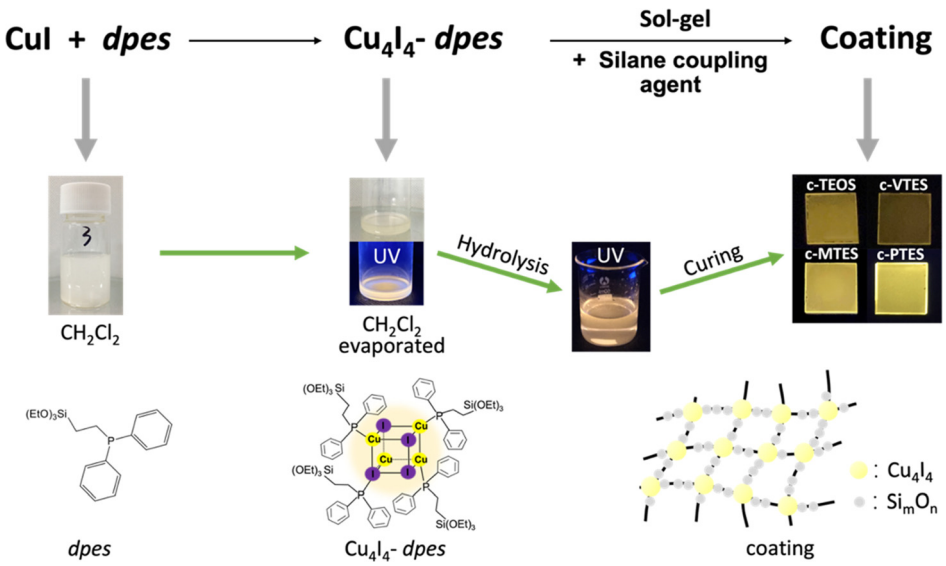

Fig. 1 Diagram of the synthetic process of the hybrid coatings.

maintain the optical properties of the precursors.[37] Under such method, the copper(I) iodide core can be effectively incorporated into multidimensional structures, forming hybrid structures that are both highly luminescent and stable.

Based on the previous studies, an efficient "bottom-up" synthetic strategy has been developed to synthesize cross-linked organic–inorganic hybrid coatings with unique luminescent properties while the emissive Cu_4I_4 core has been incorporated into the resin materials through Cu–P coordination bonds (Fig. 1).[36,38] A Cu_4I_4 based precursor, Cu_4I_4-dpes, has been synthesized by using CuI and a phosphine ligand 2-(diphenylphosphino)ethyltriethoxysilane (dpes). Then, four different kinds of such coatings (represented by **c-TEOS**, **c-VTES**, **c-MTES**, **c-PTES** respectively) have been prepared by ligand exchange of the precursor molecules Cu_4I_4-dpes with the coupling reagents of tetraethyl orthosilicate (TEOS), triethoxyvinylsilane (VTES), methyltriethoxysilane (MTES) and phenyltriethoxysilane (PTES) (Fig, S1, ESI† and Fig. 1), proving the universality of this synthetic method. In such multi-core based organic–inorganic hybrid functional coating materials, the inorganic components include both silicon oxide clusters and copper(I) iodide clusters with specific structures. The former species maintain the superior protection performance of the original hybrid resin and the high stability of the silicon-based coatings, while the latter gives the coatings superior optical properties. These hybrid coatings all emit strong yellow light under UV-light irradiation (Fig. 1). These novel hybrid materials are facile to prepare free-standing luminescent films on different substrates, displaying potential as a new type of anti-counterfeiting inks.

SEM image of the cross section of glass-based **c-PTES** prepared by spin coating (3000 rpm, 30 s) demonstrates the thickness of the coating is about 3 μm (Fig. S2, ESI†). The X-ray diffraction (XRD) analyses (Fig. 2a) show that the as-made crosslinked networks of all four coatings are totally amorphous structure. No peak of CuI is detected, indicating that CuI has been successfully incorporated into the resin structures. The Fourier transform-infrared (FT-IR) spectroscopy spectra were obtained by testing the powdery samples of coatings. As shown in Fig. 2b, each of the coatings has an obvious absorption peak at about 3418 cm^{-1}, which corresponds to intramolecularly associated –OH. The absorption peaks at about 2980 cm^{-1} and 2930 cm^{-1} correspond to the antisymmetric stretching vibrations of $-CH_3$ and $-CH_2-$. Affected by different silane coupling agents involved in the reactions, the absorption peak of **c-VTES** at 3062 cm^{-1} should correspond to the terminal C═CH, and several absorption peaks near 3072 cm^{-1} of **c-PTES** should correspond to the stretching vibrations of ═CH in the phenyl within PTES. In addition, four spectra show strong absorption peaks at about 1091 cm^{-1}, 770 cm^{-1} and 443 cm^{-1}, corresponding to the antisymmetric stretching vibration of Si–O–Si, symmetric stretching vibration of Si–O and bending vibration of Si–OH, respectively. The UV-vis absorption spectra (Fig. 2c) indicate that four coatings show no absorption in the visible light region, corresponding to their transparency as films under nature light. Their thermal stability has been evaluated by the thermogravimetric analyses, which is shown in Fig. 2d. The thermogravimetric analysis plots demonstrate that the decomposition temperature (T_D) of **c-TEOS**, **c-VTES**, **c-MTES**, and **c-PTES** are 370 °C, 406 °C, 455 °C and 400 °C, respectively.

The room temperature solid-state photoluminescence spectra of the four coating materials were recorded. As shown in Fig. 2e all four coating materials exhibit a single-band emission, with emission peaks at around 560 nm. The full width at half maximum (FWHM) of the spectra are around 120 nm. The Commission International de L' Eclairage (CIE) chromaticity coordinates (Fig. 2f) of **c-TEOS**, **c-VTES**, **c-MTES** and **c-PTES** were calculated to be (0.49, 0.48), (0.49, 0.48), (0.46, 0.49) and (0.45, 0.49) respectively, confirming their yellow light emissions. The lifetime values of **c-TEOS**, **c-VTES**, **c-MTES** and

 © 2023 The Author(s). Published by the Royal Society of Chemistry

Open Access Article. Published on 01 December 2022. Downloaded on 10/21/2025 6:40:41 AM.
This article is licensed under a Creative Commons Attribution 3.0 Unported Licence.

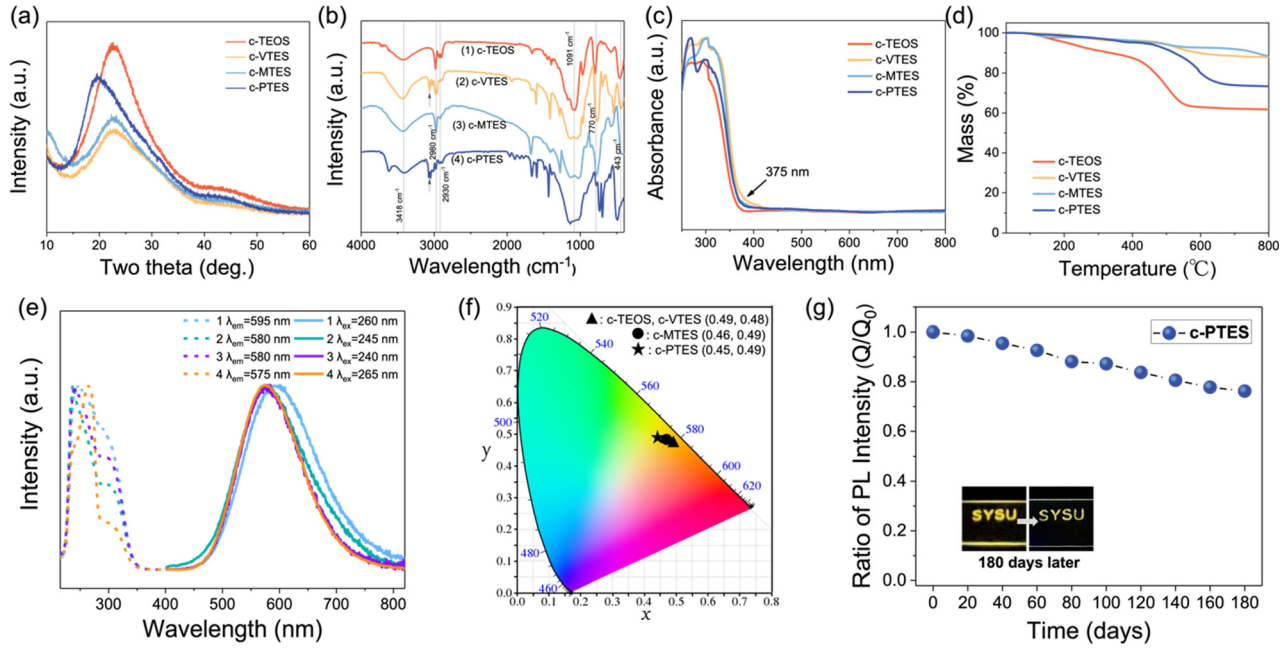

Fig. 2 (a) XRD patterns, (b) FT-IR spectra, (c) UV-vis absorption spectra and (d) TG plots of **c-TEOS**, **c-VTES**, **c-MTES**, and **c-PTES**. (e) PL excitation and emission spectra of **c-TEOS** (1), **c-VTES** (2), **c-MTES** (3), and **c-PTES** (4). (f) CIE coordinates of **c-TEOS**, **c-VTES**, **c-MTES**, and **c-PTES**. (g) Plots of PL intensity ratios of **c-PTES** over time (I_0 and I are luminescent intensity measured on day 0 and every 20 days, respectively). Insets are the images taken on day 0 and day 180 in the air under 254 nm UV irradiation.

c-PTES have been determined to be 2.93, 4.04, 6.16 and 5.99 μs by monoexponential fitting, respectively (Fig. S3, ESI†). The decay lifetimes in microseconds suggest that they are phosphorescent emission. The results are consistent with other reported Cu_4I_4 based structures.[27,34,35] The major photophysical properties of these coating materials have been summarized in Table 1. The IQYs of **c-TEOS**, **c-VTES**, **c-MTES**, and **c-PTES** are measured to be 17.6%, 24.5%, 53.3% and 57.1% respectively under 300 nm excitation, indicating that different coupling reagents affect the luminescent properties of the coatings and aromatic groups could increase emission intensity of the hybrid coatings. The stability of the coatings have been evaluated by placing the coated pattern in the air. The "SYSU" (logo pattern of Sun Yat-sen University) pattern was printed on the glass sheet, and the luminescent intensity of the pattern lost ∼20% after being placed in the moist air at room temperature for 180 days (Fig. 2g), indicating the good stability of the coating materials.

These coatings have the advantages of uniform film formation, bright luminescence, facile preparation method, low-cost and large-scale preparation, and have the potential to be the solvent-free anti-counterfeiting inks. We chose **c-PTES** with the strongest luminescence among the four coatings as the solvent-free hybrid anti-counterfeiting ink material. Screen printing is an economical and widely used thin film deposition technology, which has been commonly used in various decorative printing and flexible electronic products, biosensors, intelligent security and other fields.[39] Screen printing is applicable to various types of inks and is not limited by the size and shape of the substrate. Fig. 3a is an illustration of screen printing process. The **c-PTES** ink was poured into one end of the screen printing plate, and a certain pressure on the ink part of the screen printing plate was applied with a scraper. The scraper was moved towards the other end of the screen printing plate at a constant speed. During the movement, the ink has been pressed by the scraper from the mesh of the patterned part onto the substrate. The solvent-free **c-PTES** ink can take glass, poly(ethylene terephthalate) (PET), paper, cloth and other materials as substrates and a variety of patterns can be painted on these substrates.

After curing, the patterns emit uniform and bright yellow light under ultraviolet light of 254 nm in the dark, while they are colorless and transparent under natural light, displaying strong concealment properties (Fig. 3b). Even in the daytime, they emit distinct yellow light under ultraviolet light of 254 nm (Fig. S4, ESI†). The logo pattern of Sun Yat-sen University is printed on the transparent and flexible PET polyester film, and it can be seen that the pattern is clear and bright under UV light (Fig. S5a, ESI†). After 500 times of manual bending, there is no damage of the pattern, indicating that the printed pattern has

Table 1 Photophysical properties of the hybrid coatings

Coating	c-TEOS	c-VTES	c-MTES	c-PTES
Ex_{max} (nm)	260	245	240	265
Em_{max} (nm)	595	580	580	575
τ (μs)	2.93	4.04	6.16	5.00
CIE	(0.49, 0.48)	(0.49, 0.48)	(0.46, 0.49)	(0.45, 0.49)
IQY	17.6%	24.5%	53.3%	57.1%
T_D (°C)	370	406	455	400

Open Access Article. Published on 01 December 2022. Downloaded on 10/21/2025 6:40:41 AM.
This article is licensed under a Creative Commons Attribution 3.0 Unported Licence.

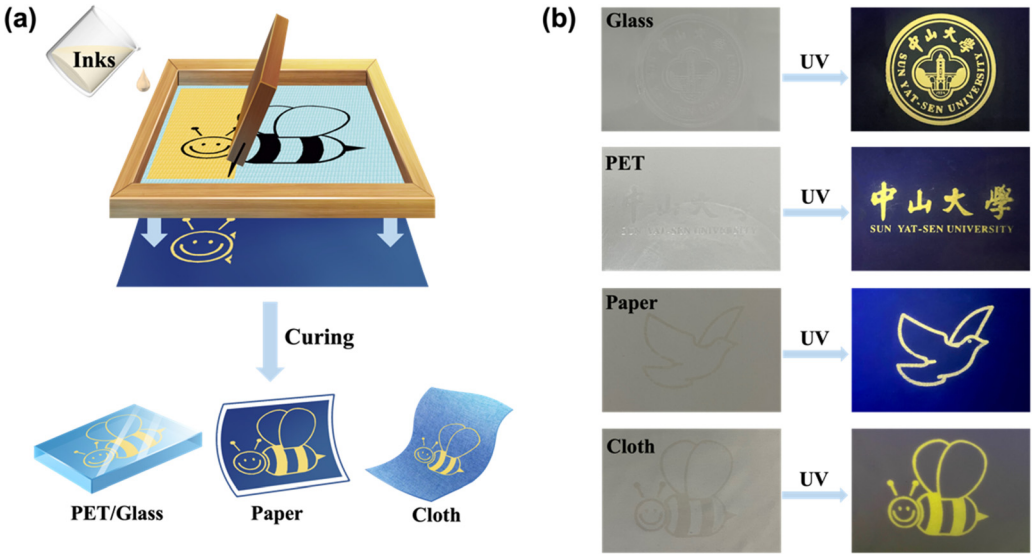

Fig. 3 (a) Schematic diagram of the process of screen printing by using hybrid luminescent anti-counterfeiting inks **c-PTES**. (b) Photos of fluorescent patterns printed on different base materials (commercial glass, PET, paper and cloth) under natural light (left) and 254 nm UV light (right).

strong mechanical performance (Fig. S5a, ESI†). The pigeon pattern printed on the paper was rubbed with eraser for 100 times, and there was no damage and no obvious change in brightness of the pattern, indicating that the printed pattern had strong friction resistance (Fig. S5b, ESI†). The water stability of anti-counterfeiting ink is also very important in the application of flexible textile anti-counterfeiting labels. As shown in Fig. S5c (ESI†), the small bee pattern printed on the textile has not been damaged or deformed after 10 times of scrubbing with detergent and water, indicating that **c-PTES** ink has excellent water and chemical stability.

Conclusions

In this work, a new type of anti-counterfeiting ink is prepared, which is very different from the traditional anti-counterfeiting inks. By synthesizing the luminescent precursor with specific structure, the crosslinked photoluminescent coating materials are obtained by the sol–gel method. In the coating structures, the light-emitting substance is combined with the cross-linked resin material through covalent bonds, so that the coatings have uniform light emission and high brightness. The hybrid coatings have the advantages of strong mechanical performance, strong water stability and friction resistance, showing the potential to be a new type of solvent-free anti-counterfeiting ink.

Author contributions

H. T. was responsible for performing all experiment; Z. Z. and Y. L. were responsible for the revision of the manuscript; H. L. was responsible for the characterization of the compounds and the editing of the manuscript; W. L. was responsible for the reviewing and editing the manuscript; G. O. was responsible for the supervision of the project, and reviewing and editing the manuscript. All authors have given approval to the final version of the manuscript.

Conflicts of interest

There are no conflicts to declare.

Notes and references

1 F. Zhang, Z. Shi, S. Li, Z. Ma, Y. Li, L. Wang, D. Wu, Y. Tian, G. Du, X. Li and C. Shan, *ACS Appl. Mater. Interfaces*, 2019, **11**, 28013–28022.
2 Y. Liu, F. Han, F. Li, Y. Zhao, M. Chen, Z. Xu, X. Zheng, H. Hu, J. Yao, T. Guo, W. Lin, Y. Zheng, B. You, P. Liu, Y. Li and L. Qian, *Nat. Commun.*, 2019, **10**, 2409.
3 R. Kwok, D. Kenny and G. A. Williams, *Forensic Sci. Int.: Genet. Suppl. Ser.*, 2019, **7**, 438–440.
4 T. P. Chou, C. Chandrasekaran, S. J. Limmer, S. Seraji, Y. Wu, M. J. Forbess, C. Nguyen and G. Z. Cao, *J. Non-Cryst. Solids*, 2001, **290**, 153–162.
5 P. Salazar-Bravo, D. Del Ángel-López, A. M. Torres-Huerta, M. A. Domínguez-Crespo, D. Palma-Ramírez and A. B. López-Oyama, *Prog. Org. Coat.*, 2019, **135**, 51–64.
6 A. Rahimi and S. Amiri, *J. Coat. Technol. Res.*, 2015, **12**, 587–593.
7 K. K. Jena, T. K. Rout, R. Narayan and K. V. S. N. Raju, *Polym. Int.*, 2012, **61**, 1101–1106.
8 M. Saveleva, A. Vladescu, C. Cotrut, L. Van der Meeren, M. Surmeneva, R. Surmenev, B. Parakhonskiy and A. G. Skirtach, *J. Mater. Chem. B*, 2019, **7**, 6778–6788.
9 R. B. Figueira, C. J. R. Silva and E. V. Pereira, *J. Coat. Technol. Res.*, 2015, **12**, 1–35.
10 Ö. Kesmez, *Chem. Pap.*, 2020, **74**, 673–688.

 © 2023 The Author(s). Published by the Royal Society of Chemistry

Open Access Article. Published on 01 December 2022. Downloaded on 10/21/2025 6:40:41 AM.
This article is licensed under a Creative Commons Attribution 3.0 Unported Licence.

11 I. J. Zvonkina and M. D. Soucek, *Curr. Opin. Chem. Eng.*, 2016, **11**, 123–127.
12 R. Goswami, *Discovery*, 2015, **29**, 201–210.
13 W. A. Zoubi, J. H. Min and Y. G. Ko, *Sci. Rep.*, 2017, **7**, 7063.
14 N. Kim, *J. Coat. Technol. Res.*, 2017, **14**, 21–34.
15 M. F. Montemor, *Surf. Coat. Technol.*, 2014, **258**, 17–37.
16 P. J. Rivero, J. A. Garcia, I. Quintana and R. Rodriguez, *Coatings*, 2018, **8**, 76.
17 S. K. Ghosh, *Functional Coatings*, 2006, pp. 1–28, DOI: 10.1002/3527608478.ch1.
18 L. Gong, F. Huang, Z. Zhang, Y. Zhong, J. Jin, K.-Z. Du and X. Huang, *Chem. Eng. J.*, 2021, **424**, 130544.
19 J.-J. Wang, C. Chen, W.-G. Chen, J.-S. Yao, J.-N. Yang, K.-H. Wang, Y.-C. Yin, M.-M. Yao, L.-Z. Feng, C. Ma, F.-J. Fan and H.-B. Yao, *J. Am. Chem. Soc.*, 2020, **142**, 3686–3690.
20 P. Kumar, S. Singh and B. K. Gupta, *Nanoscale*, 2016, **8**, 14297–14340.
21 X. Yu, H. Zhang and J. Yu, *Aggregate*, 2021, **2**, 20–34.
22 S. Zhao, M. Gao and J. Li, *J. Lumin.*, 2021, **236**, 118128.
23 J. Li, D. Xia, M. Gao, L. Jiang, S. Zhao and G. Li, *Inorg. Chim. Acta*, 2021, **526**, 120541.
24 Y. Ma, Y. Zou, Z. Zhang, J. Fang, W. Liu, Y. Ni, L. Fang, C. Lu and Z. Xu, *Cellulose*, 2020, **27**, 561–573.
25 O. Younis, E. E. El-Katori, R. Hassanien, A. S. Abousalem and O. Tsutsumi, *Dyes Pigm.*, 2020, **175**, 108146.
26 V. W.-W. Yam, V. K.-M. Au and S. Y.-L. Leung, *Chem. Rev.*, 2015, **115**, 7589–7728.
27 W. Liu, Y. Fang and J. Li, *Adv. Funct. Mater.*, 2018, **28**, 1705593.
28 R. Peng, M. Li and D. Li, *Coord. Chem. Rev.*, 2010, **254**, 1–18.
29 K. Tsuge, Y. Chishina, H. Hashiguchi, Y. Sasaki, M. Kato, S. Ishizaka and N. Kitamura, *Coord. Chem. Rev.*, 2016, **306**(Part 2), 636–651.
30 X. Hei, W. Liu, K. Zhu, S. J. Teat, S. Jensen, M. Li, D. M. O'Carroll, K. Wei, K. Tan, M. Cotlet, T. Thonhauser and J. Li, *J. Am. Chem. Soc.*, 2020, **142**, 4242–4253.
31 H. Li, Y. Lv, Z. Zhou, H. Tong, W. Liu and G. Ouyang, *Angew. Chem., Int. Ed.*, 2022, **61**, e202115225.
32 W. Liu, W. P. Lustig and J. Li, *EnergyChem*, 2019, **1**, 100008.
33 Y. Fang, W. Liu, S. J. Teat, G. Dey, Z. Shen, L. An, D. Yu, L. Wang, D. M. O'Carroll and J. Li, *Adv. Funct. Mater.*, 2017, **27**, 1603444.
34 P. C. Ford, E. Cariati and J. Bourassa, *Chem. Rev.*, 1999, **99**, 3625–3648.
35 K. R. Kyle, C. K. Ryu, P. C. Ford and J. A. DiBenedetto, *J. Am. Chem. Soc.*, 1991, **113**, 2954–2965.
36 H. Tong, H. Li, H. Li, Cidanpuchi, F. Wang and W. Liu, *Inorg. Chem.*, 2021, **60**, 15049–15054.
37 W. Liu, Y. Fang, G. Z. Wei, S. J. Teat, K. Xiong, Z. Hu, W. P. Lustig and J. Li, *J. Am. Chem. Soc.*, 2015, **137**, 9400–9408.
38 C. Tard, S. Perruchas, S. Maron, X. F. Le Goff, F. Guillen, A. Garcia, J. Vigneron, A. Etcheberry, T. Gacoin and J.-P. Boilot, *Chem. Mater.*, 2008, **20**, 7010–7016.
39 A. M. Musa, J. Kiely, R. Luxton and K. C. Honeychurch, *TrAC, Trends Anal. Chem.*, 2021, **139**, 116254.